The Mesozoic Equatorial Atlantic Magmatic Province (EQUAMP)

A New Large Igneous Province in South America

M. H. B. M. Hollanda, C. J. Archanjo, A. A. Macedo Filho, H. Fossen, R. E. Ernst, D. L. de Castro, A. C. Melo and A. L. Oliveira

Abstract Mafic dike swarms and sills intruding, respectively, the Precambrian Borborema and Paleozoic Parnaíba provinces (NE Brazil) constitute two major magmatic events related to the continental break-up that formed the Equatorial Atlantic. Available whole rock K–Ar determinations and a few plagioclase $^{40}Ar/^{39}Ar$ ages suggest that these events occurred approximately between 135 and 120 Ma. Airborne magnetic data indicates that the main dike swarm, the Rio Ceará-Mirim swarm, can be traced for about 1,000 km along an arcuate trajectory between the Cretaceous Potiguar rift near the Atlantic coastline, and the northern margin of the São Francisco craton. The dikes of the such a giant swarm form isolated (often en-echelon) segments that can reach up to 40 km in length and have a mean width of about 70 m. The sills, known as Sardinha magmatism, are intercalated between the Paleozoic sedimentary strata of the Parnaíba basin having major expression in subsurface rather than on surface. Geochemical data indicate that the parental tholeiitic magmas of dikes and sills would largely derive from melting of subcontinental lithospheric sources. However, a subordinate OIB-type component identified in some dikes would indicate contribution of a mantle plume as a melt source. In this paper we propose that the Sardinha and Rio Ceará-Mirim magmatic products, which are found over an area of about 700,000 km^2, all together represent a newly recognized Cretaceous LIP in South America here named Equatorial Atlantic Magmatic Province (EQUAMP).

M. H. B. M. Hollanda (✉) · C. J. Archanjo · A. A. Macedo Filho · A. L. Oliveira
Instituto de Geociências, Universidade de São Paulo, São Paulo 05508–080, Brazil
e-mail: hollanda@usp.br

H. Fossen
Museum of Natural History, University of Bergen, N-50, Bergen, Norway

R. E. Ernst
Department of Earth Science, Carleton University, Ottawa, Canada

R. E. Ernst
Department of Geology and Geography, Tomsk State University, 36 Lenin Ave, Tomsk 634050, Russia

D. L. de Castro · A. C. Melo
Programa de Pós-Graduação em Geodinâmica e Geofísica, Universidade Federal do Rio Grande do Norte, Natal 58078–970, Brazil

R. K. Srivastava et al. (eds.), *Dyke Swarms of the World: A Modern Perspective*, Springer Geology, https://doi.org/10.1007/978-981-13-1666-1_3

1 Introduction

During the time interval spanning the Late-Triassic to Mid-Cretaceous, one of the major continental land masses existing on Earth, the Gondwana supercontinent, was gradually dismembered into South America, Africa (Madagascar), India, Australia and Antarctica after the efficient combination of global-scale plate boundary stresses and deep mantle dynamics including mantle plumes. As a result, large igneous provinces (LIPs) (Ernst 2014) characterized by extensive mafic and/or felsic lava flows and related plumbing systems formed. Lava flows, sills and dikes are preserved in the northern Brazil, Bolivia and northwestern Africa representing part of the Triassic-Jurassic Central Atlantic Magmatic Province (CAMP; Marzoli et al. 1999a, b; Knight et al. 2004; Verati et al. 2005, 2007; Merle et al. 2011; Bertrand et al. 2014). The Cretaceous LIPs include Karoo-DML (Dronning Maud Land)-Ferrar related to the break-up of the East Gondwana involving Africa, Antarctica and Australia (183.0 ± 0.5–182.3 ± 0.6 Ma for Karoo, Svensen et al. 2012, 182.78 ± 0.03–182.43 ± 0.04 Ma for Ferrar, Burgess et al. 2015), and the Paraná-Etendeka event related to West Gondwana fragmentation to form Africa and South America in the Early Cretaceous (ca. 135 Ma; Thiede and Vasconcelos 2010; Florisbal et al. 2014; Janasi et al. 2011). At the Cretaceous-Paleogene boundary, the separation of India from the Seychelles micro-continent was intimately linked to the Deccan traps (e.g., Hooper et al. 2010; Renne et al. 2015), while the Afro-Arabian province represents the youngest LIP of Cenozoic age (30–5 Ma) along the East-African rift system (e.g., Ukstins Peate et al. 2005; Riisager et al. 2005). One common feature found in all these LIPs is the contemporaneity of the eruptive and intrusive igneous rocks emplaced either as a short-term single pulse or as multiple pulses (e.g., Courtillot et al. 2003; Ernst 2014).

Extensive flood basalt volcanism related to continental break-up is often connected to plume (or hot spot) activity, while dike swarms are at first associated with variations in the orientation and magnitude of local or regional stress fields in intraplate settings (e.g., Pollard et al. 1975). Having strike lengths in excess of 300 km, giant dike swarms are usually considered to be an important component of the plumbing system of LIPs (Ernst and Buchan 1997) and can be interpreted as sub-volcanic feeder systems of the lava flows. The spatial geometry of such giant swarms, particularly the recognition of giant radiating dike swarms (Halls 1982; Fahrig 1987) led Ernst and Buchan (1997) to propose a close link with LIPs originated by plumes, but also with either the thermal and mechanical rheology of the crustal section they are intruding, such as preexisting crustal discontinuities along with the regional stress field and its modification by domal uplift associated with mantle plume arrival at the base of the lithosphere. More recently, increasing field observations and geophysical modeling have shown that plumbing systems can also develop at very shallow levels, particularly in sedimentary basins, as extensive sill complexes (Thomson and Hutton 2004; Polteau et al. 2008; Svensen et al. 2012; Magee et al. 2016). These intrusive complexes are mapped often over several tens of kilometers and are dominated by an interconnected network of mafic dikes and sills, which frequently exhibit saucer-shaped morphologies associated with a small proportion of dikes (e.g., Muirhead et al. 2012; Magee et al. 2016). Such particular sill morphology along with lateral magma flow patterns found in regional dike swarms enable magma transport over many hundreds of kilometers and in some cases more than 2,000 km and, therefore, have broad implications for the interpretation of geochemical data obtained from large-scale magmatic areas (e.g., Meade et al. 2009). Hence, detailed structural, geophysical, geochemical and geochronological examination of giant plumbing systems (dikes plus sills) has become an essential tool to support models integrating plate tectonics and mantle dynamics in continental settings.

This paper intends to formally propose a new Cretaceous LIP in South America formed during the Equatorial Atlantic Ocean opening and, therefore, related to the break-up of the West Gondwana supercontinent. This igneous province, herein coined as Equatorial Atlantic Magmatic Province (EQUAMP), differs from other Gondwanan LIPs by encompassing dominantly (or exclusively) intrusive instead of eruptive rocks, thus satisfying the criteria for plumbing system-type continental LIPs of Bryan and Ernst (2008; also Ernst 2014) and the definition of LPPs (Large Plutonic Province) of Sheth (2007). The EQUAMP LIP consist of dikes and sills that, although having been considered as separated intrusive components in previous works, can now be investigated within the context of a single magmatic province on the basis of chemical and geochronological similarities. Some aspects of the magmatic products making up this hitherto previously unknown LIP are summarized here.

2 Geological Framework

The main EQUAMP magmatic components are the Rio Ceará-Mirim dike swarm (RCM) and the Sardinha sill province, which are intrusive into two contrasting geological settings in northeast Brazil, the Precambrian Borborema Province and the Paleozoic-Mesozoic Parnaíba Basin. The Borborema Province is a major crustal block formed by convergence between the West African and Congo-São Francisco cratons to assemble West Gondwana during the Neoproterozoic Brasiliano/Pan-African orogeny (e.g., Frimmel and Frank 1998; Caby 2003; Gray et al. 2008; Brito Neves et al. 2014). As a result of the convergence, the Borborema Province shares a number of geological features with terranes of the northwestern Africa, amongst which a dominant Paleoproterozoic gneissic-migmatitic basement, Neoproterozoic (passive margin and intracontinental) mobile belts, and voluminous (acid to mafic) plutonism dated at ca. 630–530 Ma (see Santos et al. 2010, 2014; Van Schmus et al. 2008 for a general overview of the Precambrian geology of the Borborema province). A major tectonic feature of the Brasiliano/Pan-African orogeny concerns a continental-scale network of strike-slip shear zones developed coevally with high-temperature deformation and metamorphism, and crustal anatexis (Vauchez et al. 1995; Archanjo et al. 2002a, 2013). These shear zones consist of mylonite belts that split up the Borborema Province into terranes with contrasting tectono-lithological histories, some of them accommodating late brittle fault reactivations (normal, strike-slip or locally reverse faults) related to Cambrian-Ordovician extensional events that led to the development of small intra-continental rifted basins (e.g., Sénant and Popoff 1991; Françolin et al. 1994). In the Cretaceous, the Borborema Province was affected by widespread rifting associated with the Equatorial Atlantic opening, during which the RCM and related sub-swarms and sills were emplaced.

The Neoproterozoic shear zones of the Borborema Province are covered to the west by one of the major Paleozoic sag basins of the South America, the Parnaíba Basin. The basin features a ~5-km-deep predominantly siliciclastic succession that covers approximately 600,000 km^2 overlying the Precambrian rocks of the Amazonian craton and Araguaia belt (to the west), Borborema Province (to the east) and São Francisco craton to the south (e.g., Góes and Feijó 1984). Sandstones, subordinate shales and conglomerates, as well as local limestones and evaporites, are grouped into three supersequences that record successive transgressive-regressive cycles separated by regional erosive unconformities: Silurian (Serra Grande Group), Middle Devonian-Early Carboniferous (Canindé Group) and Late Carboniferous-Early Triassic (Balsas Group) (Góes and Feijó 1984; Vaz et al. 2007). Long-term denudation of neighboring Precambrian source rocks and intrabasinal recycling were likely concurrent processes controlling the ca. 250 m.y. of sedimentation in the basin (Hollanda et al. 2018). This wide sedimentary succession, in turn, hosts two magmatic events. The older magmatic activity is represented by equivalents of the CAMP-related flood basalts (locally named Mosquito Formation; Bellieni et al. 1990; Fodor et al. 1990; Marzoli et al. 1999a; Merle et al. 2011), and the younger is represented by mafic sills and subordinate dikes grouped as the Sardinha Formation (Bellieni et al. 1990; Fodor et al. 1990). Moreover, and maybe corresponding to the lateral equivalent of the Sardinha sills, the RCM intrudes, over hundreds of kilometers in length, the Precambrian basement of the Borborema Province and the basal Silurian succession of the Parnaiba Basin.

In the following sections we outline some characteristics of the magmatic components of the EQUAMP LIP, specially their elemental and isotope geochemistry, geochronology and structural aspects. We also bring up some research issues that will be the focus of future investigations of this newly recognized magmatic province.

3 The EQUAMP Components

3.1 Dikes

In contrast to the large volumes of magma erupted during the opening of the South Atlantic, the Equatorial margin is featured by relatively modest volume of magmatism (e.g., Benkhelil 1989). The more prominent magmatic activity is the RCM dike swarm, which has long been recognized as an EW-trending swarm approximately 400 km in length and formed prior to and concurrent with the Equatorial Atlantic rifting (e.g., Matos et al. 1992, 2000). The RCM dikes are characterized by relatively thick, tholeiitic mafic bodies on the order of 20–190 m in width and 1–15 km in length (e.g., Archanjo et al. 2000, 2002b), the longer dikes being generally emplaced as en-echelon arrays. In recent years, the Brazilian Geological Survey has made available high-resolution airborne magnetic data that reveal a southwestward continuation of the RCM dikes that increases the overall swarm length by at least 600 km. The swarm changes in trend, turning from EW towards SW at approximately 38°W. Both the total length of the swarm (about 1,000 km) and its change in trend make the RCM dikes an arcuate giant swarm in the sense of Ernst and Buchan (1997). Contrasting with the well-studied dikes of the EW-trending portion, the NE-trending dikes have not yet been studied in terms of geochemical, chronological and structural aspects.

In addition to the arcuate swarm, airborne magnetic anomalies also discriminate two other sub-sets of dikes (Fig. 1). One of them is a somewhat diffuse, curved NW-trending dikes exposed nearly parallel to the Equatorial Atlantic coastline—the Canindé dike swarm, while the other is located to the southeast of the RCM swarm consisting of a NE-trending en-echelon dike system—the Riacho do Cordeiro dike swarm. This latter extends over ca. 300 km in length from the São Francisco craton to the south until intersecting with the Pernambuco lineament (Fig. 1). A local, unpublished K–Ar age of 119 ± 2 Ma in the Riacho do Cordeiro dikes suggests their temporal correlation with the RCM dikes (see the Geochronology section). As for the NE-trending portion of the RCM (NE-RCM), no petrological and age data are available for Canindé and Riacho do Cordeiro dikes.

3.2 Sills

The second EQUAMP component is the Sardinha magmatism. It consists of sheet-like bodies (sills) and local dikes that intruded the Parnaíba Basin to the east of 45°W, in the opposite side of the main area of occurrence of the CAMP lava flows (Fig. 1) (e.g., Fodor et al. 1990; Bellieni et al. 1990). Although not exclusive, the emplacement of sills as seen in the field is dominantly controlled by rheological differences between the host-rock lithologies of the Canindé Group, i.e. along the contact between the regressive-transgressive sedimentary successions. A recent study combining seismic, magnetic and surface geologic data showed that the occurrence of both CAMP and Sardinha magmatic events are much more extensive in subsurface than those mapped on surface (Mocitaiba et al. 2017). An integrated modeling using geochemical (major element) and geophysical (magnetic susceptibility) data suggest that the CAMP magmatism is not restricted to the west (and to the south) areas, but might occur to the east interstratified with Sardinha sills (de Castro et al. 2018).

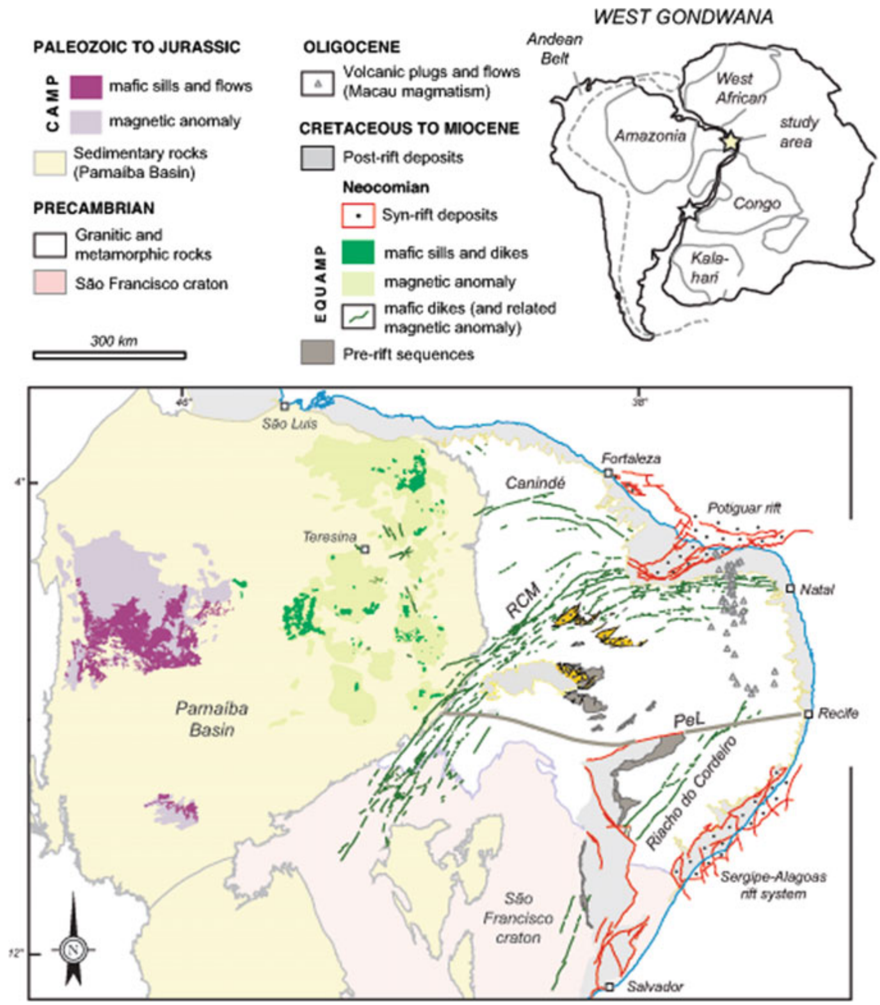

Fig. 1 Simplified map integrating the Borborema Province and Parnaíba Basin. Dikes that are associated to the Rio Ceará-Mirim magmatic event are shown as green lines. The Sardinha magmatic event is mostly represented by sills within the basin; the dark green areas are the exposures of sills on surface, while the light green areas illustrate the subsurface distribution based on geophysical data (after Mocitaiba et al. 2017). The remnant CAMP flood basalts are highlighted in dark purple (surface exposures) and light purple (subsurface interpretation). The inset on the top is a schematic picture of West Gondwana and related cratonic blocks, with location of the study area. RCM refers to the Rio Ceará-Mirimdikeswarm and PeL refers to the Pernambuco Lineament, whereas PEMP (see inset) is the abbreviation to Paraná-Etendeka Magmatic Province

3.3 Size of the Dike Swarm

Physical parameters (length and width) of the RCM dike swarm were determined using Google Earth™ imagery combined with regional magnetic anomalies map. The semi-arid environment of NE Brazil offers good contrast between mafic dikes and their host granite-gneissic rocks, with dikes forming well-defined dark, ribbon-like patches cutting across the fabric of the Precambrian basement. As the regional relief is nearly flat along dike exposures and most these occur as vertical bodies, dimensions measured on satellite image approach to their real length and thickness. Image sources provided by Google Earth™ in the NE Brazil combines Spot Image scenes acquired between 2011 and 2012 and Digital Globe Imagery (LANDSAT 7 and 8) acquired from 2002 to 2010. Image resolution is typically about 15 m per pixel, which means that mafic dikes below about 30 m in width and 100 m in length become increasingly difficult to detect on Google Earth™. Hence, the study on dike dimensions is focussed mostly to the larger RCM dikes. Some dikes with widths lower than 30 m included on Table 1 were identified in field work.

Dikes of the EW- and NE-trending portions of the RCM dike swarm are mostly linear consisting of simple isolated bodies or arrays of two or more dike segments connected by steps. Both simple and connected dike segments show left- or right-lateral en-echelon arrangements on satellite image. In a few places where vertical sections are available, the dike walls are vertical or show steep dips. We did not observe steps connecting dikes in vertical sections, although they are necessary to interconnect the dike system from their more continuous underlying sources up to the actual level of exposure. Columnar joints resulting from shrinkage on cooling were not detected, although such features, if present, may have been masked by the common onion-skin weathering that affect the mafic dikes. Furthermore, and possibly due to pervasive physical alteration that usually mask the contact between dikes and their wall-rocks, chilled margins were recorded in just a few dikes.

Dike length (L) was estimated by measuring the distance between the most remote points on the dikes exposure. When connected by steps, the length is the total distance between the most remote points of the dike array. Widths were measured perpendicular to dike wall and its maximum width (Wm) refers to the widest segment recorded on the satellite image. Lengths of 71 dike segments of the EW-RCM range from 0.1 to 14.8 km (mean $L = 3.3$ km). On the other hand, maximum widths range from 18 to 193 m (mean $Wm = 84.7$ m). Similar dimensions are recorded in dikes of the NE-trending portion (NE-RCM). Their lengths vary from 0.4 to 37.7 km (mean $L = 4.9$ km) with widths that vary from 16.5 to 193 m (mean $Wm = 68.3$ m). In a logarithmic $L - Wm$ diagram (Fig. 2) the RCM dikes plot above the Oligocene mafic dike swarm that intrudes the extended Precambrian crust of East Africa (Schultz et al. 2008) and radial composite dikes distributed around an eroded volcanic neck intrusive in shallow crust of North America (Shiprock dikes; Delaney and Pollard 1981). RCM and Ethiopian dike swarms show equivalent dike lengths, and both are longer than Shiprock dikes. However, the RCM dikes are thicker than Ethiopian and Shiprock dikes, which we attribute to the deeper crustal exposure of the RCM dikes compared to those swarms.

Table 1 Length (L) and maximum width (Wm) of single dikes and dikes connected by steps of the Rio Ceará Mirim dike swarm (geographic coordinates in decimal degrees)

E-trending sub-swarm single dike		L (m)	Wm (m)	E-trending sub-swarm connected dike		L (m)	Wm (m)	NE-trending sub-swarm single dike		L (m)	Wm (m)	NE-trending sub-swarm connected dike		L (m)	Wm (m)
−5.580729	−36.063835	1568.6	100.9	−5.582922	−36.106884	2371.8	109.8	−5.515651	−38.898315	3627.3	84.1	−5.478237	−38.658944	9110	130.6
−5.586941	−36.143577	686.1	59.8	−5.586154	−36.126771	1413.9	96.5	−5.479401	−38.638361	2736.2	83.8	−5.562484	−39.025787	3690.2	108.7
−5.586059	−36.155305	1453.7	96.7	−5.584593	−36.310338	1954.2	80.4	−5.653879	−39.149624	1897	78.8	−5.611699	−39.089268	6651.6	124.5
−5.582604	−36.325942	378.3	62.8	−5.586278	−36.490779	2246.2	70.3	−5.669289	−39.169342	1957.5	70.5	−6.522031	−40.159948	2534.4	48.9
−5.581192	−36.333218	780.9	75.4	−5.615733	−36.135447	4337.1	77.6	−5.720268	−39.215706	708.5	67.5	−5.704575	−39.207428	4929.4	84.5
−5.583323	−36.340984	706.7	65.7	−5.605185	−36.175568	3234.9	38	−5.746920	−39.234538	674.5	43.4	−5.792078	−39.276657	3705.1	101.7
−5.583684	−36.346782	326.9	46.2	−5.631748	−36.214467	3542.1	159.9	−5.750573	−39.237466	397.4	35.3	−6.535719	−40.130091	2733.1	75.1
−5.582820	−36.349681	173.5	44.7	−5.628287	−36.260285	2968.8	112	−5.757382	−39.245056	2008.3	59.8	−6.508134	−40.211957	15625.7	62.8
−5.581147	−36.359331	1194.8	97	−5.628834	−36.298031	5821.5	146.9	−5.922960	−39.395905	833.9	31	−6.449727	−40.137205	4478.7	51.8
−5.588746	−36.379231	999.9	80.5	−5.628308	−36.348808	3862.5	90.3	−5.950754	−39.438298	1252.2	56.6	−6.616423	−40.243631	13593.1	193.1
−5.586448	−36.390985	479.2	73.8	−5.623948	−36.430519	9736.7	165.4	−5.963765	−39.467555	2643	83.7	−6.178690	−38.831951	2464.7	57.5
−5.581983	−36.401008	622.7	62.6	−5.629994	−36.503285	2255.5	131.4	−6.419035	−40.010023	4259.5	82.3	−5.768205	−38.906234	7318.9	78.2
−5.578341	−36.413192	1243.6	40.3	−5.636220	−36.528466	2895.7	115.5	−6.444844	−40.128876	2952.8	55.1	−5.818030	−38.999919	1621.6	20.3
−5.586691	−36.483759	545.7	62.6	−5.652184	−36.597987	8558.8	154.8	−6.582735	−40.275499	2903.3	33.1	−7.615401	−41.279334	7595.4	52.9
−5.586969	−36.508836	678.5	64.5	−5.654612	−36.759833	6382.3	97.5	−6.655130	−40.396479	6019.5	91.4	−7.744713	−41.354655	10573.8	82.5
−5.590312	−36.715075	1267.5	67.5	−5.712730	−36.200267	14785.2	82.7	−6.656107	−40.390006	4142.1	47.9				
−5.591448	−36.725798	1008.4	52.5	−5.694811	−36.390401	6492.3	54.5	−6.565351	−40.160537	6444.2	53.9				
−5.626569	−36.102989	2083.5	74.7	−5.707974	−37.005634	8541.4	193.5	−6.807680	−40.013111	5959.8	116.4				
−5.621491	−36.150741	4040.4	88.1	−5.702631	−37.061279	4796.6	170.9	−6.008898	−38.704992	1539.5	77.8				
−5.622041	−36.167189	2101.3	61.3	−5.706217	−37.081675	3289.9	107.3	−6.025138	−38.725893	4093.8	109.7				

(continued)

Table 1 (continued)

E-trending sub-swarm single dike		L (m)	Wm (m)	E-trending sub-swarm connected dike		L (m)	Wm (m)	NE-trending sub-swarm single dike		L (m)	Wm (m)	NE-trending sub-swarm connected dike		L (m)	Wm (m)
−5.626001	−36.184523	2932	101.8	−5.702291	−37.127776	11606.3	46.6	−6.092764	−38.776757	6651.7	105.1				
−5.623021	−36.390696	2032	107.1	−5.705699	−37.206947	7973.7	40.6	−5.686260	−38.697981	37744.4	84.3				
−5.639188	−36.546479	2088.7	108.5	−5.721650	−37.122460	4961.2	65.8	−6.145310	−38.811325	893.3	38.8				
−5.651099	−36.673277	2014.4	128.6	−5.726393	−37.138106	7684.2	69.5	−6.212479	−38.863307	4176.1	59.1				
−5.651418	−36.689752	1728	99.5	−5.760599	−37.273365	10731.9	110.9	−5.721989	−38.764520	2125.6	16.5				
−5.654194	−36.712985	1368.2	70.4	−5.759746	−37.293428	3782.7	120	−5.730039	−38.790512	1835.9	33.1				
−5.692279	−36.330835	439	44.2	−5.757640	−37.333447	4822.6	146.9	−5.741068	−38.831904	5771	68.3				
−5.693060	−36.333754	100.9	41.4	−5.767072	−37.383816	8048.9	129.2	−5.812867	−38.972914	1224.8	29.4				
−5.695595	−36.354311	2124.7	42.4	−5.764409	−36.972563	2891.9	69.8	−5.802497	−38.972086	1039.8	21.6				
−5.695944	−36.357476	1156.5	27.1	−5.784362	−37.186460	11338.8	69.7	−5.823231	−39.012125	1038.7	17.9				
−5.699989	−36.527563	1714.1	104.4					−6.792033	−40.562761	2761.5	73.1				
−5.702113	−36.574401	2307.2	40.3					−6.825990	−40.595860	14827.4	67.4				
−5.702919	−36.583349	2575.9	62.6					−7.013061	−40.867360	2239.9	59.6				
−5.707797	−36.615090	2873.2	52					−7.630816	−41.305865	1531.1	28.1				
−5.670239	−36.794425	7620.9	104					−7.754221	−41.416877	1111.8	31.3				
−5.674502	−36.836615	2365.3	134.4					−7.803599	−41.489832	3918.6	106.2				
−5.731334	−36.826275	1709	67.7					−7.823625	−41.519608	3820.6	86.5				
−5.779134	−37.036340	1608.7	30					−7.850077	−41.548152	3148.8	45.5				
−5.776622	−37.151489	3553.4	64.4					−7.872843	−41.572725	5014.8	78.2				
−5.584905	−36.356969	170	25					−7.945703	−41.641504	14978.5	70.2				
−5.795622	−37.769662	313	60												

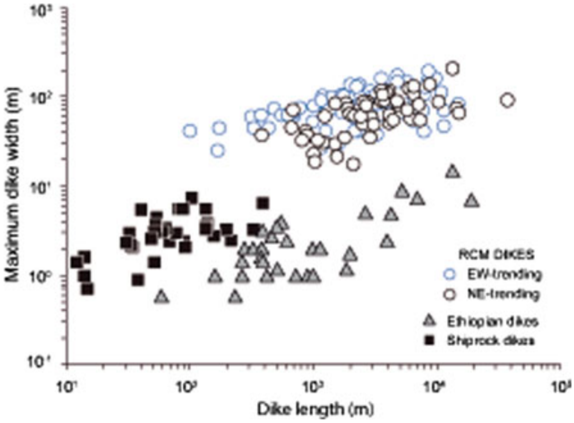

Fig. 2 Relationship between the length (L) and maximum width (Wm) for mafic dikes of the RCM dike swarm (see details in the text). Data from Shiprock dikes and Ethiopian mafic swarm are available in Delaney and Pollard (1981) and Schultz et al. (2008)

3.4 AMS Data from RCM Dikes

According to Archanjo et al. (2002b) and Archanjo and Launeau (2004), normal-type anisotropy of magnetic susceptibility (AMS) fabrics of the EW-RCM dikes are consistent with a lateral magma flow along the central and western sectors of the swarm. AMS magnitude is weak, mostly between 2 and 5%, and provided by multidomain titanomagnetite grains. In contrast, the low-field magnetic susceptibility of the mafic dikes is strong, about 10^{-2} SI, which is consistent with the intensity of the aeromagnetic anomalies that define the trace of the dikes in the regional maps. To investigate the relationship between the opening of fissures to emplace the basaltic magma and the orientation of magnetic fabric we sampled two mafic dikes for which the wall-rock contacts are exposed in field. These dikes are situated in the middle and western part of the EW-RCM dike swarm and are respectively, 18 m (CM30) and 150 m (CM43) in width. Although the susceptibility and anisotropy parameters of these samples have already been published in Archanjo et al. (2002b), we introduce here a new interpretation of AMS based on the obliquity between the dike fabric and the wall-rock orientation (Fig. 3).

Shape ellipsoids vary from oblate to prolate in one dike (CM30) and are dominantly oblate in the other (CM43). Strongly prolate ellipsoids ($T < -0.5$) indicate a linear fabric while oblate ellipsoids ($T > 0.5$) indicate a planar fabric. The majority of samples in one dike (CM30) shows dominant prolate ellipsoids, with lineations oblique (samples F, G, H and I) to a high angle (A, C) to the dike wall. In samples with neutral ($T \sim 0$) to oblate ($T > 0$) ellipsoids, the foliations tend to be perpendicular to the dike plane; one sample (D) shows a well-defined foliation ($T = 0.66$) nearly parallel to the dike.

In the larger dike (CM45), the magnetic foliations typically are oblique to the dike trend. The strike of the magnetic foliation is usually in a NE-SW directions and dips are variable, but usually steep to the NW or SE. Lineations, in contrast, tend to disperse to different directions in agreement with the oblate shape of the AMS ellipsoids. The magnetic fabric that transects the dike, and particularly the foliation

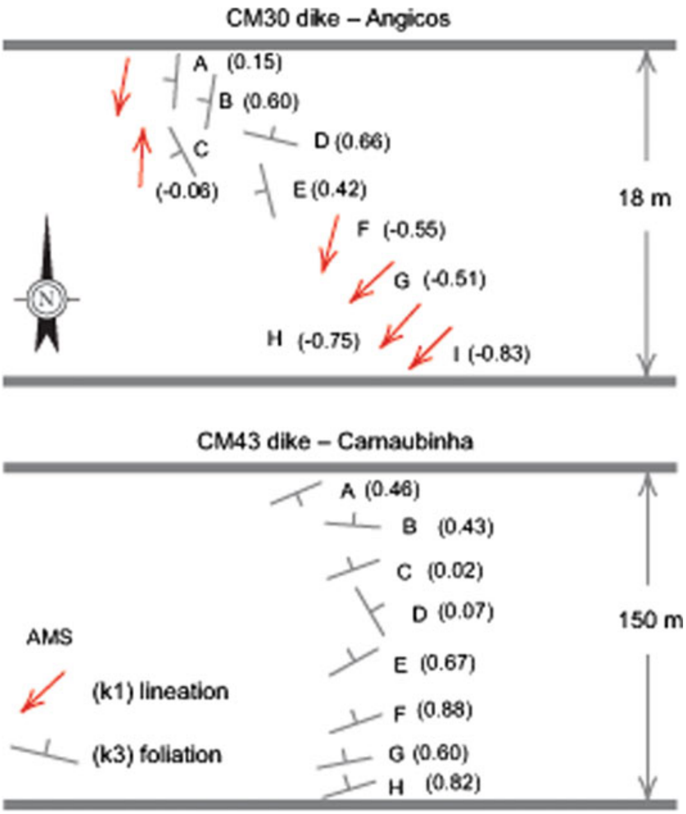

Fig. 3 Anisotropy of magnetic susceptibility (AMS) of two dikes (CM30 and CM45) whose contacts are exposed with the host regional rocks. Magnetic fabric of dike CM30 shows prolate (T < 0) and oblate (T > 0) AMS shape ellipsoids while oblate fabrics dominate the AMS fabric in the dike CM45. Oblique to highly-oblique lineations in the dike with neutral to prolate ellipsoids (CM30) and well-defined asymmetrical magnetic foliations in the larger dike (CM45) suggest that the fracture opening that accommodated the mafic magma included a component of lateral strike slip displacement parallel to the dike wall. Note: capital letters refer to the measurement site and respective AMS shape parameter (value given in parentheses) (see details in the text)

along the larger dike, would be formed by the combined influence of magma flux and syn-emplacement shearing before magma freezing (Correa-Gomes et al. 2001; Féménias et al. 2004; Clemente et al. 2007). The AMS of the dike with neutral to prolate ellipsoids (CM30) would be carried by needle-like titanomagnetite grains that would grow preferentially along the principal direction of local extension (Knight and Walker 1988). Late magmatic shearing parallel to the dike wall, in turn, would provide a transected magnetic foliation in the thicker dike. AMS results suggest, therefore, that the opening of fractures that accommodated the EW-RCM dikes combined a component of normal dilatation and a component of lateral strike slip offset of the wall-rocks.

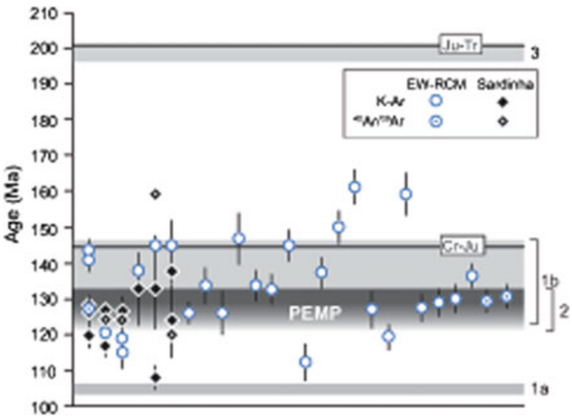

Fig. 4 K–Ar and $^{40}Ar/^{39}Ar$ ages available in the literature for the EQUAMP diabases (see sources in the text). Gray areas are shown for comparison: (1a, 1b) Northern Benue Trough ($^{40}Ar/^{39}Ar$ ages—Maluski et al. 1995); (2) Paraná-Etendeka ($^{40}Ar/^{39}Ar$ ages—Renne et al. 1992, 1996a, b; Raposo et al. 1998; Ernesto et al. 1999; Marzoli et al. 1999a, b; Mincato 2000; Thiede and Vasconcelos 2010; U–Pb ages—Janasi et al. 2011; Florisbal et al. 2014; Almeida et al. 2017); and (3) CAMP-Parnaíba ($^{40}Ar/^{39}Ar$ ages—Baksi and Archibald 1997; Marzoli et al. 1999a; Merle et al. 2011)

4 Geochronology

Diabases of the EW-RCM dikes and Sardinha sill magmatic events have been dated since the 90s using the K–Ar method (Bellieni et al. 1990, 1992; Fodor et al. 1990; Misusaki et al. 2002), while only a few $^{40}Ar/^{39}Ar$ ages were published for the sills (Baksi and Archibald 1997) and dikes (Smith et al. 2001; Ngonge et al. 2016a) (Fig. 4). The ages are mainly scattered between 160 and 110 Ma, although younger and older K–Ar ages are also reported. Paleomagnetic data obtained from diabases of the EW-RCM showed that the dikes were emplaced at different times and under reverse and normal geomagnetic polarities, but with magnetization directions acquired mainly in the Early Cretaceous (the sub-swarms I, II, IV and V of Bellieni et al. 1992). Conversely, another set of dikes gave paleopoles corresponding to the Jurassic (the sub-swarm II). The authors suggest that the different magnetic signatures of the EW-RCM dikes, would reflect rifting processes related to the opening of the Equatorial (Cretaceous) and Central (Jurassic) domains of the Atlantic Ocean. If the duration of the RCM magmatic event as revealed by the K–Ar ages is trustworthy, this would imply that the dike swarm was emplaced over a time span of at least 55 m.y. and, therefore, would represent one longer-lasting magmatic activity when compared to other Gondwanan LIPs (ca. 135 Ma Paraná-Etendeka and 200 Ma CAMP) in South America. This lifetime is approximately coeval with the volcanic and plutonic activity in the Benue Trough (Maluski et al. 1995; Coulon et al. 1996), which is thought to be the African failed rift of a triple junction linked to the Atlantic opening (e.g., Matos 1992, 2000).

Defining the timing and duration of LIPs requires a precise and accurate geochronological survey that certainly does not involve the use of the K–Ar system. This is mainly because of limitations in recognizing either Ar loss or excess radiogenic Ar, which can lead to age misinterpretations. Taking into account only the $^{40}Ar/^{39}Ar$ results available for both sills and dikes, the EQUAMP lifespan would be nearly coincident with the main peak of the Paraná-Etendeka (flood lavas and intrusives) magmatic activity, between 135 and 120 Ma. Nevertheless, the poor precision associated to the current dataset of ages makes still difficult to determine the time span of the EQUAMP. Hence, much remains to be done to constrain the temporal history of the EQUAMP LIP.

5 Petrological Aspects

The data available for the EW-RCM and the Sardinha magmatic events reveal that both are dominantly represented by fine- to medium-grained, tholeiitic basalts and basaltic andesites, while the RCM dikes also includes trachy-basalts and basaltic trachy-andesites (Bellieni et al. 1990, 1992; Fodor et al. 1990; Hollanda et al. 2006; Ngonge et al. 2016a) (Fig. 5a, b). Plagioclase, two pyroxenes (augite and pigeonite) and Fe–Ti oxides make up the main mineral assemblage, while olivine occurs as a main constituent in some dikes of the EW-RCM dikes or as very subordinate minerals in Sardinha sills.

The EQUAMP dikes are dominantly (~80% vol.) high-Ti tholeiites with $MgO < 5$ wt% and $TiO_2 \geq 1.5$ wt% ($Ti/Y \sim 360$), whereas low-Ti tholeiites ($TiO_2 \leq 1.5$ wt%; $Ti/Y \leq 360$) and a set of high-Ti olivine tholeiitic dikes are minor components (Fig. 5c, d). Tholeiites of intermediate and acid compositions are absent in the EW-RCM dikes. The Sardinha intrusives, in turn, have been described essentially as high-Ti tholeiites ($MgO < 5$ wt% and $TiO_2 \geq 2$ wt%; Bellieni et al. 1990; Fodor et al. 1990), while low-Ti tholeiitic diabases would represent a minor component. As aforementioned, it should be acknowledged the current uncertainty in distinguishing sills belonging to Sardinha and/or CAMP events at the east side of the Parnaíba Basin. In general, both RCM and Sardinha tholeiites are strongly affected by fractional crystallization.

The distinction in terms of enrichment in incompatible trace elements between the three tholeiite groups of the EW-RCM follows the Ti-based definition, i.e. the evolved high-Ti tholeiites have higher incompatible element (Rb, Ba, Th, U, LREE, Sr, Zr, Hf) contents relative to the low-Ti tholeiites, whereas the olivine tholeiites are lesser enriched (Ngonge et al. 2016a). A negative Nb–Ta anomaly is more prominent in the low-Ti tholeiites than in the evolved high-Ti tholeiites, contrasting with the OIB-type abundances found for the olivine tholeiites. Such contrasting trace element signatures are evidence for a non-parentage relationship between the olivine tholeiitic and the other magma types. In fact, the initial ($t \sim 130$ Ma) isotopic compositions of the olivine tholeiites reveal likely contribution of a FOZO-type asthenospheric component ($^{87}Sr/^{86}Sr = 0.70339$–$0.70373$, $^{143}Nd/^{144}Nd = 0.512518$–$0.512699$ and $^{206}Pb/^{204}Pb > 19.1$; Ngonge et al. 2016a), while the high- and low-Ti tholeiites have

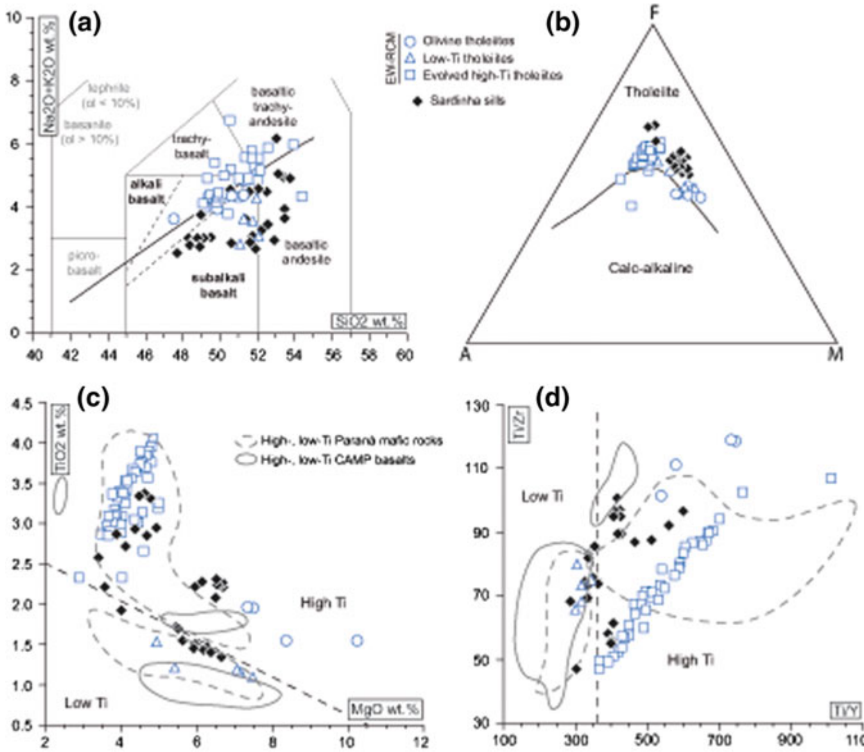

Fig. 5 Total oxide and element contents of the EQUAMP tholeiites from database of the literature (Bellieni et al. 1990, 1992; Fodor et al. 1990; Hollanda et al. 2006; Ngonge et al. 2016a). **a** Total alkali-silica (TAS) diagram after (Le Maitre 2002); **b** AFM (Alkalis–FeO–MgO) plot with the dividing line of Irvine and Baragar (1971); **c** TiO_2–MgO and **d** Ti/Y–Ti/Zr variation diagrams. Fields of Paraná-Etendeka (Peate 1997; Rocha-Júnior et al. 2013) and CAMP-Parnaíba (Bellieni et al. 1990; Fodor et al. 1990; Merle et al. 2011) are shown for comparison

variable Sr–Nd and relatively non-radiogenic $^{206}Pb/^{204}Pb$ initial ratios indicating that the primary melts of the RCM magmas were segregated from a heterogeneous EM1-type mantle (Hollanda et al. 2006; Ngonge et al. 2016a). The low-Ti magmas, however, display some degree of crustal contamination.

Although not studied to the same level of detail as the EW-RCM dikes, the geochemical signature of the Mg-evolved, Sardinha tholeiites is also featured by enrichment in incompatible elements and a negative Nb anomaly. From the current geochemical information and the (very limited) isotope dataset (i.e., radiogenic Sr, and non-radiogenic Nd and Pb compositions), the origin of the Sardinha parental magmas has been attributed to variable degrees of melting of an enriched and strongly heterogeneous, spinel-garnet peridotite source (Bellieni et al. 1990; Fodor et al. 1990; Silva et al. 2017).

6 Discussion

6.1 Dike Physical Parameters and AMS Data

The RCM swarm, before restricted to EW-trending dikes situated to the south of the Potiguar rift, has increased dramatically in length based on mapping from high-resolution aeromagnetic data collected for northeast Brazil. To the west, the swarm changes its direction to reach, to the south of Permanbuco Lineament, the border of the São Francisco craton (Fig. 1). According to aeromagnetic and remote sensing criteria, the arcuate RCM dikes can be traced for about 1,000 km in length, hence defining a giant dike swarm. The mafic dikes appear as isolated, en-echelon segments sometimes connected by steps in map view. Mean lengths of these segments reach 3.3 and 4.7 km in the EW- and NE-trending portions, whereas maximum widths range from 60 to 80 m, respectively. The thickness of the RCM mafic dikes are, therefore, higher than those in the Ethiopian swarm, which is emplaced in a rifting setting. We can speculate that the RCM dikes would be closer to their reservoirs compared to the Ethiopian dikes, although the relation between dike thickness and geological setting needs further investigation.

According to Archanjo et al. (2000, 2002b), AMS studies in the EW-RCM dikes indicated a possible feeder zone located in the east sector of the swarm. Such a feeder zone was characterized by vertical magnetic lineations found at the intersection of the dike swarm and the Cenozoic volcanic centers of the Macau magmatism (Fig. 1; Ngonge et al. 2016b). In contrast, AMS of the central and west sectors of the EW-trending swarm indicates lateral flow of magma that, in some cases, may include magnetic fabrics of tectonic origin, i.e. formed in the final stages of crystallization of the melt in a distensive stress field. Transected magnetic foliations recorded in some dikes are suggestive of a lateral (strike slip) displacement of the host-rock walls which, in turn, would indicate that the mode I-type fracture opening that assisted the emplacement of the dikes would include a component of shearing. These structural findings, observed just in the EW-trending portion of the swarm, have to be compared to AMS of the NE-RCM dikes in order to propose a consistent regional tectonic model for the crustal fracturing and intrusion of dikes. Moreover, a detailed AMS investigation is required in the connection of the RCM and Canindé swarms since they regionally form a radial arrangement whose focus appears to be centered next to the Cretaceous Potiguar rift (see Fig. 1). A modeled geoid anomaly in NE Brazil indicates a low-density (thermal) zone situated at between 17 and 78 km in depth (Ussami et al. 1993), which agrees with our estimated melting depths (between 60 and 75 km; Ngonge et al. 2016a) for the RCM tholeiites, i.e., in the garnet-spinel facies of the transition zone.

6.2 Preliminary Comparison with the ca. 135 Ma Paraná-Etendeka

Taking into account that a complete geochemical survey is still unavailable for the entire RCM dikes and Sardinha sills, a comparison between EQUAMP and the approximately coeval Paraná-Etendeka LIP can only be made at some extent. The Paraná-Etendeka LIP is located approximately 1,500 km to the south of the exposed area of the EQUAMP (Fig. 1, inset), being asymmetrically split into South America (southern Brazil) and Africa (Namibia and Angola). The volcanic rocks are mainly tholeiitic basalts and basaltic andesites, with subordinate occurrence of silicic rocks that span the dacite-trachyte-rhyolite compositional fields (e.g., Piccirillo and Melfi 1988; Peate et al. 1992; Ewart et al. 1998a, b, 2004a, b; Nardy et al. 2008). From the published ages, the Paraná-Etendeka volcanism began at ca. 135 Ma and lasted 133–132 Ma (see references in Fig. 4), although ages attributed to the related plumbing systems can progress up to 131 Ma (Raposo et al. 1998; Mincato 2000). Flood basalt lavas and associated intrusive rocks are geochemically classified into low-Ti and high-Ti types based on an arbitrary threshold of 2 wt% of TiO_2 content with corresponding Ti/Y values of ~330–350 (e.g., Peate et al. 1992). On both the Brazilian side, these two major chemical groups are spread into two areas referenced as southern (dominated by low-Ti lavas and some dike swarms) and northern (dominated by high-Ti lavas, sills and dikes) domains, whereas one central domain brings together both geochemical groups. Conversely, high- and low-Ti rocks of the EQUAMP are not geographically controlled and, at least from the current knowledge, the low-Ti types are very subordinate relative to those of high-Ti compositions, representing only 10% of volume of the EW-RCM dikes, while even more subordinate in the Sardinha sills.

The two igneous provinces are formed under nearly similar tectonic frameworks. Paraná-Etendeka lavas and Sardinha sills of EQUAMP were formed, respectively, by flooding and intruding Paleozoic sag-type basins, while the RCM and the subsidiary Canindé and Riacho do Cordeiro swarms of EQUAMP are intrusive into the Precambrian basement, as well as a number of dike swarms related to the Paraná-Etendeka LIP (e.g., Ponta Grossa, Florianópolis, São Paulo-Rio de Janeiro and their equivalents in the African side; e.g., Renne et al. 1996a; Deckart et al. 1998; Raposo et al. 1998; Marzoli et al. 1999b; Florisbal et al. 2014; Almeida et al. 2017; Raposo 2017). The spatial distribution of dike swarms in both these provinces suggests a triple junction configuration developed during the stepwise opening of the South Atlantic in the Cretaceous. The intimate association of triple junction geometry and with voluminous and short-lived magmatism as seen for the Paraná-Etendeka LIP is strongly suggestive of plume-related provinces, whether the plume had participated as an active source for melt generation or providing heat to trigger melting of the lithospheric mantle. Differences in Ti contents in the Paraná magmas are followed by distinctive major and trace element concentrations and isotope compositions, and they have been explained as a function of either heterogeneities in their lithospheric mantle sources (e.g., Milner et al. 1995; Peate 1997; Marzoli et al.

1999b; Rocha-Júnior et al. 2012, 2013) or plume (Tristan)-lithosphere interactions (e.g., Gibson et al. 1995; Ewart et al. 1998a, b; Thompson et al. 2001). No definitive OIB compositions has been reported for the flood lavas of the Paraná-Etendeka LIP, hence favoring the idea of Tristan plume was mainly a heat instead a melt source.

Chemical mantle heterogeneity is also an explanation for the coexistence of high- and low-Ti compositions in the RCM and Sardinha tholeiites of the EQUAMP (Fodor et al. 1990; Ngonge et al. 2016a). Based on the correlation between negative Nb-anomaly, incompatible element enrichment and isotope modeling, a subduction-modified subcontinental lithospheric mantle has been proposed as the more likely source for the Cretaceous magmatism in NE Brazil. As the ultimate pre-Andean subduction history in the South America dates back the Brasiliano/Pan-African orogeny, which was accounted for the convergence of major cratonic blocks and ocean consumption to assembly the West Gondwana at the Ediacaran-Cambrian. Subduction-related metasomatism might be certainly an ubiquitous signature preserved in the lithospheric mantle beneath the Precambrian terranes in South America. Melt production from potentially enriched lithospheric mantle reservoir will mainly depend on the rheology and fertility of the lithosphere, partial melting degree, and the thermal gradient of the heat source. Otherwise, evidence for OIB-type (FOZO-like) signature shown by the olivine tholeiitic dikes of the EW-RCM suggests that a deep mantle source has also contributed with melt provenance during the Equatorial Atlantic geodynamic evolution.

Given the current level of understanding about petrogenesis of the Gondwanan LIPs in South America, the 135 Ma Paraná-Etendeka, 200 Ma CAMP and even the 'newborn' ca. 130 Ma EQUAMP, much remains to be investigated concerning to the extent of partial melting, crust assimilation and fractional crystallization processes in governing the compositional variations observed in continental basalts from these provinces. As a direct consequence of obtaining such information, the contribution of lithosphere and convective (asthenosphere or plume) mantle reservoirs can be determined. Future investigations on the EQUAMP tholeiites will be focused on quantitative and numerical modeling based on a priori trace element and isotope data in order to define the nature and the thermomechanical conditions of the sub-continental mantle beneath NE Brazil during the breakup of the Gondwana along the Equatorial Atlantic margin.

7 Conclusions

We have reviewed the evidence from two magmatic suites in NE Brazil—mafic sills which are intrusive in the Parnaíba Basin and dike swarms located mostly in the Precambrian basement of the Borborema Province. We propose the dikes and sills comprise a new Cretaceous LIP in South America, which we are labeling as the EQUAMP (EQUatorial Atlantic Magmatic Province). The approximate ages of ca. 135–120 Ma suggest a close association with the opening of the Equatorial Atlantic, making the study of this LIP a thought-provoking subject in the context of supercontinent cycle. The relationship with the approximately coeval ca. 135 Ma Parana-Etendeka LIP centred about 1,500 km further south, also requires investigation.

Acknowledgements The authors Maria Helena B. M. Hollanda, Carlos J. Archanjo and David L. de Castro thanks to the Conselho Nacional de Pesquisa e Desenvolvimento (CNPq) for grants 304979/2016-3, 305824/2014-7 and 303015/2013-6, respectively. Antomat A. Macedo, Alanny C. C. Melo and Alisson L. Oliveira thanks to FAPESP and CAPES, respectively, for their PhD scholarships. REE was partially supported from Mega-Grant 14.Y26.31.0012 of the government of the Russian Federation. The authors are grateful to the referees (Dr. David Peate and Dr. Elson Oliveira) for the comments and corrections that helped to improve the final version of the manuscript. This paper is the first scientific contribution funded by FAPESP 2017/08423-9.

References

Almeida VV, Janasi VA, Heaman LM, Shaulis BJ, Hollanda MHBM, Renne PR (2017) Contemporaneous alkaline and tholeiitic magmatism in the Ponta Grossa Arch Paraná-Etendeka Magmatic Province: constraints from U-Pb zircon/baddeleyite and $^{40}Ar/^{39}Ar$ phlogopite dating of the José Fernandes Gabbro and mafic dikes. J Volcanol Geoth Res (accepted). https://doi.org/10.1016/j.volgeores.2017.01.018

Archanjo CJ, Launeau P (2004) Magma flow inferred from preferred orientations of plagioclase of the Rio Ceará-Mirim dike swarm (NE Brazil) and its AMS significance. In: Martin-Hernandez F, Lunemburg CM, Aubourg C, Jackson M (eds) Magnetic fabric: methods and applications. Geological Society, London, Special Publications, vol 238, pp 285–298. https://doi.org/10.1144/gsl.sp.2004.238.01.17

Archanjo CJ, Trindade RIF, Macedo JWP, Araújo MGS (2000) Magnetic fabric of a basaltic dike swarm associated with Mesozoic rifting in northeastern Brazil. J S Am Earth Sci 13:179–189. https://doi.org/10.1016/S0895-9811(00)00023-7

Archanjo CJ, Trindade RI, Bouchez JL, Ernesto M (2002a). Granite fabrics and regional-scale strain partitioning in the Seridó belt (Borborema Province, NE Brazil). Tectonics. https://doi.org/10.1029/2000tc001269

Archanjo CJ, Araújo MGS, Launeau P (2002b) Fabric of the Rio Ceará-Mirim mafic dike swarm (Northeastern Brazil) determined by anisotropy of magnetic susceptibility and image analysis. J Geophys Res 107(B3):1–13, 2046. https://doi.org/10.1029/2001jb000268

Archanjo CJ, Viegas LG, Hollanda MHBM, Souza LC, Liu D (2013) Timing of the HT/LP transpression in the Neoproterozoic Seridó belt (Borborema Province, Brazil): constraints from U-Pb (SHRIMP) geochronology and implications for the connections between NE Brazil and West Africa. Gondwana Res 23:701–714. https://doi.org/10.1016/j.gr.2012.05.005

Baksi AK, Archibald DA (1997) Mesozoic igneous activity in the Maranhão province, northern Brazil: $^{40}Ar/^{39}Ar$ evidence for separate episodes of basaltic magmatism. Earth Planet Sci Lett 151(3–4):139–153

Bellieni G, Piccirillo EM, Cavazzini G, Petrini R, Comin-Chiaramonti P, Nardy AJR, Civetta L, Melfi AJ, Zantedeschi P (1990) Low- and high-TiO_2 Mesozoic tholeiitic magmatism of the Maranhão basin (NE-Brasil): K-Ar age, geochemistry, petrology, isotope characteristics and relationships with Mesozoic low- and high-TiO_2 flood basalts of the Paraná basin (SE-Brazil). Neues Jahrbuch Miner Abh 162(1):1–33

Bellieni G, Macedo MHF, Petrini R, Picirillo EM, Cavazzini G, Comin-Chiaramonti P, Ernesto M, Macedo JWP, Martins G, Melfi AJ, Pacca IG, De Min J (1992) Evidence of magmatic activity related to Middle Jurassic to early cretaceous rifting from northeastern Brazil (Ceará-Mirim): K/Ar age, palaeomagnetism, petrology and Sr-Nd isotope characteristics. Chem Geol 97:9–32

Benkhelil J (1989) The origin and evolution of the cretaceous Benue trough (Nigeria). J Afr Earth Sci 8(2/3/4):251–282

Bertrand H, Fornari M, Marzoli A, García-Duarte R, Sempere T (2014) The Central Atlantic Magmatic Province extends into Bolivia. Lithos 188:33–43. https://doi.org/10.1016/j.lithos.2013.10.019

Brito Neves BB, Fuck RA, Pimentel MM (2014) The Brasiliano collage in South America: a review. Braz J Geol 44(3):493–518. https://doi.org/10.5327/Z2317-48892014000300010

Bryan S, Ernst RE (2008) Revised definition of Large Igneous Provinces (LIPs). Earth Sci Rev 86:175–202. https://doi.org/10.1016/j.earscirev.2007.08.008

Burgess SD, Bowring SA, Fleming TH, Elliot DH (2015) High-precision geochronology links the Ferrar large igneous province with early-Jurassic ocean anoxia and biotic crisis. Earth Planet Sci Lett 415:90–99. https://doi.org/10.1016/j.epsl.2015.01.037

Caby R (2003) Terrane assembly and geodynamic evolution of central-western Hoggar: a synthesis. J Afr Earth Sci 37:133–159. https://doi.org/10.1016/j.afrearsci.2003.05.003

Clemente CS, Amorós EB, Crespo MG (2007) Dike intrusion under stress: effects on magnetic and vesicle fabrics in dikes from rift zones of Tenerife (Canary Islands). J Struct Geol 29:1931–1942. https://doi.org/10.1016/j.jsg.2007.08.005

Correa-Gomes LC, Souza Filho CR, Martins CFJN, Oliveira EP (2001) Development of symmetrical and asymmetrical fabric in sheet-like igneous bodies: the role of magma flow and wall-rock displacements in theoretical and natural cases. J Struct Geol 23:1415–1428. https://doi.org/10.1016/S0191-8141(01)00007-4

Coulon C, Vidal P, Dupuy C, Baudin P, Popoff M, Maluski H, Hermitte D (1996) The Mesozoic to early Cenozoic magmatism of the Benue trough (Nigeria); geochemical evidence for the involvement of the St Helena plume. J Petrol 37:341–358. https://doi.org/10.1093/petrology/37.6.1341

Courtillot V, Davaille A, Besse J, Stock J (2003) Three distinct types of hotspots in the Earth's mantle. Earth Planet Sci Lett 205:295–308

Deckart K, Féraud G, Marques LS, Bertrand H (1998) New time constraints on dike swarms related to the Paraná-Etendeka magmatic province, and subsequent South Atlantic opening, southeastern Brazil. J Volcanol Geoth Res 80:67–83. https://doi.org/10.1016/S0377-0273(97)00038-3

de Castro DL, Oliveira DC, Hollanda MHBM (2018) Geostatistical interplay between geophysical and geochemical data: mapping litho-structural assemblages of Mesozoic igneous activities in the Parnaíba Basin (NE Brazil). Surv Geophys 39:683–713. https://doi.org/10.1007/s10712-018-9463-5

Delaney PT, Pollard DD (1981) Deformation of host rocks and flow of magma during growth of minette dikes and breccia-bearing intrusions near Ship Rock, New Mexico. US Geol Surv Prof Pap 1202:61p

Ernesto M, Raposo MIB, Marques LS, Renne PR, Diogo LA, de Min A (1999) Paleomagnetism, geochemistry and $^{40}Ar/^{39}Ar$ dating of the northeastern Paraná Magmatic Province: tectonic implications. J Geodyn 28:321–340. https://doi.org/10.1016/S0264-3707(99)00013-7

Ernst RE (2014) Large Igneous Province. Cambridge Un Press, United Kingdom, 653 pp

Ernst RE, Buchan KL (1997) Giant radiating dike swarms: their use in identifying pre-Mesozoic large igneous provinces and mantle plumes. AGU Geophys Monogr 100:297–333

Ewart A, Milner SC, Armstrong RA, Duncan AR (1998a) Etendeka volcanism of the Goboboseb Mountains and Messum Igneous complex, Namibia. Part I: Geochemical evidence of Early Cretaceous Tristan plume melts and the role of crustal contamination in the Parana-Etendeka CFB. J Petrol 39:191–225. https://doi.org/10.1093/petroj/39.2.191

Ewart A, Milner SC, Armstrong RA, Duncan AR (1998b) Etendeka volcanism of the Goboboseb Mountains and Messum Igneous Complex, Namibia. Part II: voluminous quartz latite volcanism of the Awahab magma system. J Petrol 39:227–253. https://doi.org/10.1093/petroj/39.2.227

Ewart A, Marsh JS, Milner SC, Duncan AR, Kamber BS, Armstrong RA (2004a) Petrology and geochemistry of Early Cretaceous bimodal continental flood volcanism of the NW Etendeka, Namibia. Part 1: introduction, mafic Lavas and re-evaluation of mantle source components. J Petrol 45:59–105. https://doi.org/10.1093/petrology/egg083

Ewart A, Marsh JS, Milner SC, Duncan AR, Kamber BS, Armstrong RA (2004b) Petrology and geochemistry of Early Cretaceous bimodal continental flood volcanism of the NW Etendeka, Namibia. Part 2: Characteristics and petrogenesis of the high-Ti latite and high-Ti and low-Ti voluminous quartz latite eruptives. J Petrol 44:107–138. https://doi.org/10.1093/petrology/egg082

Féménias O, Diot H, Berza T, Gauffriau A, Demaiffe D (2004) Asymmetrical to symmetrical magnetic fabric of dikes: paleo-flow orientations and paleo-stresses recorded on feeder-bodies from the Motru Dike Swarm (Romania). J Struct Geol 26:1401–1418. https://doi.org/10.1016/j.jsg.2003.12.003

Florisbal LM, Heaman LM, Janasi VA, Bitencourt MF (2014) Tectonic significance of the Florianópolis dike swarm, Paraná-Etendeka Magmatic Province: a reappraisal based on precise U-Pb dating. J Volcanol Geoth Res 289(2014):140–150. https://doi.org/10.1016/j.jvolgeores.2014.11.007

Françolin JBL, Cobbold PR, Szatmari P (1994) Faulting in the early cretaceous Rio do Peixe basin (NE Brazil) and its significance for the opening of the Atlantic. J Struct Geol 16(5):647–661. https://doi.org/10.1016/0191-8141(94)90116-3

Frimmel HE, Frank W (1998) Neoproterozoic tectono-thermal evolution of the Gariep Belt and its basement, Namibia and South Africa. Precambr Res 90:1–28. https://doi.org/10.1016/S0301-9268(98)00029-1

Fahrig WF (1987) The tectonic setting of continental mafic dike swarms: failed arm and early passive margin. In Halls HC, Fahrig WF (eds) Mafic dike swarms. Geological Association of Canada, Special Publication, St John's, NL, vol 34, pp 331–348

Fodor RV, Sial AN, Mukasa SB, McKee EH (1990) Petrology, isotope characteristics, and K-Ar ages of the Maranhão, northern Brazil, Mesozoic basalt province. Contrib Miner Petrol 104:555–567

Gibson SA, Thompson RN, Dickin AP, Leonardos OH (1995) High-Ti and low-Ti mafic potassic magmas: key to plume-lithospheric interactions and continental flood-basalt genesis. Earth Planet Sci Lett 136:149–165. https://doi.org/10.1016/0012-821X(95)00179-G

Góes AMO, Feijó FJ (1984) Bacia do Parnaíba. Boletim de Geociências da Petrobras 8(3):57–67

Gray DR, Foster DA, Meert JG, Goscombe BD, Armstrong R, Trouw RAJ, Passchier CW (2008) A Damara orogen perspective on the assembly of southwestern Gondwana. In: Pankhurst RJ, Trouw RAJ, Brito Neves BB, De Wit MJ (eds), West Gondwana: pre-cenozoic correlations across the South Atlantic Region. Geological Society of London, Special Publications, vol 294, pp 399–412. https://doi.org/10.1144/sp294.5

Knight MD, Walker GPL (1988) Magma flow directions in dikes of the Koolau Complex, Oahu, determined from magnetic fabric studies. J Geophys Res 93:4301–4319. https://doi.org/10.1029/JB093iB05p04301

Halls HC (1982) The importance and potential of mafic dike swarms in studies of geodynamic process. Geosci Can 9:145–154

Hollanda MHBM, Pimentel MM, Oliveira DC, Jardim de Sá EF (2006) Lithosphere-asthenosphere interaction and the origin of cretaceous tholeiitic magmatism in Northeastern Brazil: Sr–Nd–Pb isotopic evidence. Lithos 86:34–49. https://doi.org/10.1016/jlithos.2005.04.004

Hollanda MHBM, Góes AN, Negri FA (2018) Sedimentary provenance of sandstones of the Parnaíba Basin through detrital zircon geochronology. In: Daly MC, Fuck RA, Julià J, Watts AB, Andrade V (eds) Cratonic basin formation: a case of the Parnaíba Basin of Brazil. Geological Society, London, Special Publications, 472. https://doi.org/10.1144/SP472.16

Hooper P, Widdowson M, Kelley S (2010) Tectonic setting and timing of the final Deccan flood basalt eruptions. Geology 38(9):839–842. https://doi.org/10.1130/G31072.1

Irvine TN, Baragar WRA (1971) A guide to the chemical classification of the common volcanic rocks. Can J Earth Sci 8:523–548

Janasi VA, Freitas VA, Heaman LH (2011) The onset of flood basalt volcanism, Northern Paraná Basin, Brazil: a precise U-Pb baddeleyite/zircon age for a Chapecó-type dacite. Earth Planet Sci Lett 302(1–2):147–153. https://doi.org/10.1016/j.epsl.2010.12.005

Knight KB, Nomade S, Renne PR, Marzoli A, Bertrand H, Youbi N (2004) The Central Atlantic Magmatic Province at the Triassic-Jurassic boundary: paleomagnetic and $^{40}Ar/^{39}Ar$ evidence from Morocco for brief, episodic volcanism. Earth Planet Sci Lett 228:143–160. https://doi.org/10.1016/j.epsl.2004.09.022

Le Maitre RW (2002) Igneous rocks—a classification and glossary of terms. In: Recommendations of the IUGS subcommission on the systematics of igneous rocks, 2nd edn. Cambridge University Press, Cambridge

Magee C, Muirhead JD, Karvelas A, Holford SP, Jackson CAL, Bastow ID, Schoeld N, Stevenson CTE, McLean C, McCarthy W, Shtukert O (2016) Lateral magma flow in mafic sill complexes. Geosphere 12(3):809–841. https://doi.org/10.1130/GES01256.1

Maluski H, Coulon C, Popoff M, Baudin P (1995) $^{40}Ar/^{39}Ar$ chronology, petrology and geodynamic setting of Mesozoic to early Cenozoic magmatism from the Benue trough, Nigeria. J Geol Soc Lond 152:311–326. https://doi.org/10.1144/gsjgs.152.2.0311

Marzoli A, Renne PR, Piccirillo EM, Ernesto M, Bellieni G, De Min A (1999a) Extensive 200-million-year-old continental flood basalts of the Central Atlantic Magmatic Province. Science 284:616–618. https://doi.org/10.1126/science.284.5414.616

Marzoli A, Melluso L, Morra V, Renne PR, Sgrosso I, D'Antonio M, Duarte Morais L, Morais EAA, Ricci G (1999b) Geochronology and petrology of Cretaceous basaltic magmatism in the Kwanza basin (western Angola), and relationships with the Paraná-Etendeka continental flood basalt province. J Geodyn 28:341–356. https://doi.org/10.1016/s0264-3707(99)00014-9

Matos RMD (1992) The northeast Brazilian rift system. Tectonics 11(4):766–791. https://doi.org/10.1029/91TC03092

Matos RMD (2000) Tectonic evolution of the Equatorial South Atlantic. In: Webster M, Talwani M (eds) Atlantic rifts and continental margins, American Geophysical Union, vol 115, pp 331–354

Meade FC, Chew DM, Troll VR, Ellam RM, Page L (2009) Magma ascent along a major terrane boundary: crustal contamination and magma mixing at the Drumadoon intrusive complex, Isle of Arran, Scotland. J Petrol 50:2345–2374. https://doi.org/10.1093/petrology/egp081

Merle R, Marzoli A, Bertrand H, Reisberg L, Verati C, Zimmermann C, Chiaradia M, Belienni G, Ernesto M (2011) $^{40}Ar/^{39}Ar$ ages and Sr-Nd-Pb-Os geochemistry of CAMP tholeiites from Western Maranhão basin (NE Brazil). Lithos 122:137–151. https://doi.org/10.1016/j.lithos.2010.12.010

Milner SC, Duncan AR, Whittingham AM, Ewart A (1995) Trans-atlantic correlation of eruptive sequences and individual silicic volcanic units within the Paraná-Etendeka igneous province. J Volcanol Geoth Res 69:137–157. https://doi.org/10.1016/0377-0273(95)00040-2

Mincato RL (2000) Metalogenia dos elementos do grupo da Platina com base na estratigrafia e geoquímica da Província Ígnea Continental do Paraná. Ph.D. thesis, Universidade de Campinas, São Paulo, 172 pp

Misusaki AMP, Thomaz-Filho A, Milani EJ, Césero P (2002) Mesozoic and Cenozoic igneous activity and its tectonic control in Northeastern Brazil. J S Am Earth Sci 15:183–198. https://doi.org/10.1016/S0895-9811(02)00014-7

Mocitaiba LSR, de Castro DL, Oliveira DC (2017) Cartografia geofísica regional do magmatismo mesozoico na Bacia do Parnaíba. Geologia USP Série Científica 17(2):169–192. https://doi.org/10.11606/issn.2316-9095.v17-455

Muirhead JD, Airoldi G, Rowland JV, White JDL (2012) Interconnected sills and inclined sheet intrusions control shallow magma transport in the Ferrar large igneous province, Antarctica. Geol Soc Am Bull 124(1/2):162–180. https://doi.org/10.1130/B30455.1

Nardy AJR, MAchado FB, Oliveira MAF (2008) As rochas vulcânicas mesozóicas ácidas da Bacia do Paraná: litoestratigrafia e considerações geoquímico-estratigráficas. Revista Brasileira de Geociências 38(1):178–195

Ngonge ED, Hollanda MHBM, Archanjo CJ, Oliveira DC, Vasconcelos PMP, Muñoz PRM (2016a) Petrology of continental tholeiitic magmas forming a 350-km-long Mesozoic dike swarm in NE Brazil: constraints of geochemical and isotopic data. Lithos 258–259:228–252. https://doi.org/10.1016/j.lithos.2016.04.008

Ngonge ED, Hollanda MHBM, Pimentel MM, Oliveira DC (2016b) Petrology of the alkaline rocks of the Macau Volcanic Field, NE Brazil. Lithos 206–207:453–470. https://doi.org/10.1016/j.lithos.2016.10.008

Peate DW (1997) The Paraná-Etendeka province. In: Large igneous provinces: continental, oceanic and planetary flood volcanism. AGU Geophysical Monographs, vol 100, pp 217–245

Peate DW, Hawkesworth CJ, Mantovani MSM (1992) Chemical stratigraphy of the Paraná lavas (South America): classification of magma types and their spatial distribution. Bull Volc 55:119–139

Piccirillo EM, Melfi AJ (1988) The Mesozoic flood volcanism of the Paraná Basin: petrogenetic and geophysical aspects. Universidade de São Paulo, São Paulo, 600 pp

Pollard DD, Müller OH, Dockstader DR (1975) The form and growth of fingered sheet intrusions. Geol Soc Am Bull 86(3):351–363

Polteau S, Mazzini A, Galland O, Planke S, Malthe-Sørenssen A (2008) Saucer-shaped intrusions: occurrences, emplacement and implications. Earth Planet Sci Lett 266:195–204. https://doi.org/10.1016/j.epsl.2007.11.015

Raposo MIB (2017) Magnetic fabrics of the Cretaceous dike swarms from São Paulo coastline (SE Brazil): its relationship with South Atlantic Ocean opening. Tectonophysics. https://doi.org/10.1016/j.tecto.2017.10.023

Raposo MIB, Ernesto M, Renne PR (1998) Paleomagnetism and dating of the early Cretaceous Florianópolis dike swarm (Santa Catarina Island), Southern Brazil. Phys Earth Planet Inter 108:275–290. https://doi.org/10.1016/S0031-9201(98)00102-2

Renne PR, Ernesto M, Pacca IG, Coe RS, Glen JM, Prevot M, Perrin M (1992) The age of Paraná flood volcanism, rifting of Gondwanaland, and the Jurassic-Cretaceous boundary. Science 258:975–979. https://doi.org/10.1126/science.258.5084.975

Renne PR, Deckart K, Ernesto M, Féraud G, Piccirillo EM (1996a) Age of the Ponta Grossa dike swarm (Brazil), and implications to Paraná flood volcanism. Earth Planet Sci Lett 144:199–211. https://doi.org/10.1016/0012-821X(96)00155-0

Renne PR, Glen JM, Milner SC, Duncan AR (1996b) Age of Etendeka flood volcanism and associated intrusions in southwestern Africa. Geology 24:659–662. https://doi.org/10.1130/0091-7613(1996)024.00659

Renne PR, Sprain CJ, Richards MA, Self S, Vanderkluysen L, Pande K (2015) State shift in Deccan volcanism at the Cretaceous-Paleogene boundary, possibly induced by impact. Science 350(62556):76–78. https://doi.org/10.1126/science.aac7549

Riisager P, Knight KB, Baker JA, Ukstins Peate I, Al-Kadasi M, Al-Subbary A, Renne PR (2005) Paleomagnetism and ^{40}Ar/^{39}Ar geochronology of Yemeni Oligocene volcanics: implications for timing and duration of Afro-Arabian traps and geometry of the Oligocene paleomagnetic field. Earth Planetary Sci Lett 237:647–672. https://doi.org/10.1016/j.epsl.2005.06.016

Rocha-Júnior ERV, Putchel IS, Marques LS, Walker RJ, Machado FB, Nardy AJR, Babinski M, Figueiredo AMG (2012) Re-Os isotope and highly siderophile element systematics of the Paraná continental flood basalts (Brazil). Earth Planet Sci Lett 337–338:164–173. https://doi.org/10.1016/j.epsl.2012.04.050

Rocha-Júnior ERV, Marques LS, Babinski M, Nardy AJR, Figueiredo AMG, Machado FB (2013) Sr–Nd–Pb isotopic constraints on the nature of the mantle sources involved in the genesis of the high-Ti tholeiites from northern Paraná Continental Flood Basalts (Brazil). J S Am Earth Sci 46:9–25. https://doi.org/10.1016/j.jsames.2013.04.004

Santos EJ, Van Schmus WR, Kozuch M, Brito Neves BB (2010) The Cariris Velhos tectonic event in Northeast Brazil. J S Am Earth Sci 29:61–76. https://doi.org/10.1016/j.jsames.2009.07.003

Santos EJ, Souza Neto JA, Silva MRR, Beurlen H, Cavalcanti JAD, da Silva MG, Dias VM, Costa AF, Santos LCML, Santos RB (2014) Metalogênese das porções norte e central da Província Borborema. In: Silva MG, Rocha Neto MB, Jost H, Kuyumijan RM (eds) Metalogênese das Províncias Tectônicas Brasileiras, pp 343–388

Sénant J, Popoff M (1991) Early cretaceous extension in Northeast Brazil related to the South Atlantic opening. Tectonophysics 198:35–46. https://doi.org/10.1016/0040-1951(91)90129-G

Schultz RA, Mège D, Diot H (2008) Emplacement conditions of igneous dikes in Ethiopian traps. J Volcanol Geoth Res 178:683–692. https://doi.org/10.1016/j.jvolgeores.2008.08.012

Sheth HC (2007) 'Large Igneous Provinces (LIPs)': definition, recommended terminology, and a hierarchical classification. Earth Sci Rev 85:117–124. https://doi.org/10.1016/j.earscirev.2007.07.005

Silva AG, Almeida CN, Valente SC, Almeida LFB (2017) The petrogenesis of tholeiitic diabases in eastern Parnaíba Basin: evidence for geochemical heterogeneities in the subcontinental lithospheric mantle in NE Brazil. Braz J Geol 47(1):109–126. https://doi.org/10.1590/2317-4889201720160041

Smith PE, Evensen NM, York D, Szatmari P, Oliveira DC (2001) Single crystal ^{40}Ar-^{39}Ar dating of pyrite: no fool's clock. Geology 29:403–406. https://doi.org/10.1130/0091-7613(2001)029

Svensen H, Corfu F, Polteau S, Hammer Ø, Planke S (2012) Rapid magma emplacement in the Karoo Large Igneous Province. Earth Planet Sci Lett 325–326:1–9. https://doi.org/10.1016/j.epsl.2012.01.015

Thiede D, Vasconcelos PM (2010) Paraná flood basalts: rapid extrusion hypothesis confirmed by new ^{40}Ar/^{39}Ar results. Geology 38(8):747–750. https://doi.org/10.1130/G30919.1

Thompson RN, Gibson SA, Dickin AP, Smith PM (2001) Early cretaceous basalt and picrite dikes of the Southern Etendeka region, NW Namibia: windows into the role of the Tristan mantle plume in Paraná-Etendeka magmatism. J Petrol 42:2049–2081. https://doi.org/10.1093/petrology/42.11.2049

Thomson K, Hutton D (2004) Geometry and growth of sill complexes: insights using 3D seismic from the North Rockall Trough. Bull Volc 66:364–375. https://doi.org/10.1007/s00445-003-0320-z

Ukstins Peate I, Baker JA, Al-Kadasi M, Al-Subbary A, Knight KB, Riisager P, Thirlwall MF, Peate DW, Renne PR, Menzies MA (2005) Volcanic stratigraphy of large-volume silicic pyroclastic eruptions during Oligocene Afro-Arabian flood volcanism in Yemen. Bull Volc 68:135–156. https://doi.org/10.1007/s00445-005-0428-4

Ussami N, Sá NC, Molina EC (1993) Gravity Map of Brazil II: regional and residual gravity anomalies and their a correlation with major tectonic provinces. J Geophys Res 98:2199–2208

Van Schmus WR, Oliveira EP, Silva Filho AF, Toteu SF, Penaye J, Guimarães IP (2008) Proterozoic links between the Borborema Province, NE Brazil, and the Central African Fold Belt. In: Pankhurst RJ, Trouw RAJ, Brito Neves BB, De Wit MJ (eds) West Gondwana: pre-cenozoic correlations across the South Atlantic Region. Geological Society of London, Special Publications, vol 294, pp 69–99. https://doi.org/10.1144/sp294.5

Vauchez A, Neves S, Caby R, Corsini M, Egydio-Silva ME, Arthaud M, Amaro V (1995) The Borborema Province shear zone system. J S Am Earth Sci 8(3/4):247–266. https://doi.org/10.1016/0895-9811(95)00012-5

Vaz PT, Rezende NGAM, Wanderley Filho JR, Travassos WAS (2007) Bacia do Parnaíba. Boletim de Geociências DA Petrobras 15(2):253–263

Verati C, Bertrand H, Féraud G (2005) The farthest record of the Central Atlantic Magmatic Province into West Africa craton: Precise $^{40}Ar/^{39}Ar$ dating and geochemistry of Taoudenni basin intrusives (northern Mali). Earth Planet Sci Lett 235:391–407. https://doi.org/10.1016/j.epsl.2005.04.012

Verati C, Rapaille C, Féraud G, Marzoli A, Bertrand H, Youbi N (2007) $^{40}Ar/^{39}Ar$ ages and duration of the Central Atlantic Magmatic Province volcanism in Morocco and Portugal and its relation to the Triassic-Jurassic boundary. Palaeogeogr Palaeoclimatol Palaeoecol 244(2007):308–325. https://doi.org/10.1016/j.palaeo.2006.06.033